Sensors and Actuators A 181 (2012) 70–76

Contents lists available at SciVerse ScienceDirect

Sensors and Actuators A: Physical

journal homepage: www.elsevier.com/locate/sna

# Equivalent circuit modeling of ionomer and ionic polymer conductive network composite actuators containing ionic liquids

Yang Liu[a], Ran Zhao[a], Mehdi Ghaffari[b], Junhong Lin[b], Sheng Liu[a], Hülya Cebeci[c], Roberto Guzmán de Villoria[c], Reza Montazami[d], Dong Wang[e], Brian L. Wardle[c], James R. Heflin[e], Q.M. Zhang[a,b,*]

[a] Department of Electrical Engineering, Pennsylvania State University, University Park, PA 16802, United States
[b] Department of Materials Science and Engineering, Pennsylvania State University, University Park, PA 16802, United States
[c] Department of Aeronautics and Astronautics, Massachusetts Institute of Technology, Cambridge, MA 02139, United States
[d] Department of Mechanical Engineering, Iowa State University, Ames, IA 50011, United States
[e] Department of Physics, Virginia Tech, Blacksburg, VA 24061, United States

ARTICLE INFO

*Article history:*
Received 21 August 2011
Received in revised form 1 May 2012
Accepted 2 May 2012
Available online 10 May 2012

*Keywords:*
Ionic electro-active polymers (*i*-EAPs)
Ionic polymer actuators
Equivalent circuit models
Warburg diffusion

ABSTRACT

In this study, we demonstrate electrical equivalent circuits that model the complex frequency-dependent impedance of 1-ethyl-3-methylimidazolium trifluoromethanesulfonate (EMI-Tf) containing electro-active polymer membranes and ionic polymer conductor network composite (IPCNC) devices. The devices include Nafion membrane actuators, Nafion coated with layer-by-layer (LbL) Au nanoparticle/poly(allylamine hydrochloride) (PAH) composite actuators, and Nafion with vertically aligned carbon nanotube (VA-CNT)/Nafion composite actuators. It is found that the low frequency responses of these devices indicate Warburg diffusion. Therefore, Warburg impedance is utilized to model the low frequency diffusion behavior of the devices, while the electric double layer capacitance ($C_{dl}$) represents the storage of drifting ions under electric field at high frequencies. It is found that $C_{dl}$ for Nafion with 40 wt% EMI-Tf is 7.5 μF/cm$^2$ and increases to 11.4 μF/cm$^2$ with increasing surface area of the LbL composite electrode. $C_{dl}$ increases further to above $3 \times 10^3$ μF/cm$^2$ for an actuator with 12 μm VA-CNT/Nafion composite electrodes, while the Warburg coefficient $A_W$ remains nearly the same for all the devices. As a result, the actuation magnitude and speed increase with charges accumulated due to higher $C_{dl}$, without much increase in the contribution from the slow ion diffusion process.



## 1. Introduction

Due to their low operation voltages (∼ a few volts) and large strain responses (∼10%), ionic electroactive polymer (*i*-EAP) actuators such as ionic polymer metal composites (IPMC) and conducting polymer actuators are attractive for many electromechanical applications [1–5]. Recently, it has been demonstrated that using ionic liquids (ILs) in *i*-EAP actuators can lead to improved device performance [2,3,6,7]. For example, the negligible vapor pressure of ILs enables ionic devices to operate at ambient atmosphere with long life cycles (∼$10^5$) [6]; the wide electrochemical window allows higher voltages (3–6 V) than that of using aqueous electrolytes and hence improves strain magnitude; and the higher ion mobility can lead to faster device response. Since the early 2000s, ionic polymer conductor network composite (IPCNC) actuators with device operation principle analogous to that of IPMC and with ILs as the electrolytes have been investigated. [6–8] Fig. 1(a) and (b) schematically present typical device configurations for electroactive devices including an IL-containing membrane with planar electrodes and a 5-layer structure that consists of an IL-containing membrane and large surface area composite electrodes. While the ionomer membrane actuators in Fig. 1(a) offer simple structure for easy device fabrication and material analysis, the two nano-composite electrodes in the 5-layer devices (such as IPMC and IPCNC) provide large specific electrode area for ion storage under an applied voltage which enhances the bending actuation. As shown in Fig. 1(c), under electrical stimulus, the excess ions drift and diffuse into/out of the two composite electrodes and therefore swell/shrink the electrode regions, consequently causing bending actuation. On the other hand, introducing a strain to these devices (such as IPMC and IPCNC) can also generate electric signal which allows them to be used as sensors [1,4,5,9–12].

The actuation response of these actuators is affected by the ion transport and the elastic coupling between ions and ionomers (in Fig. 1(a)) and the composite materials (in Fig. 1(b)). As illustrated

* Corresponding author at: N219 Millennium Science Complex, University Park, PA 16802, United States. Tel.: +1 814 863 8994; fax: +1 814 863 7846.
*E-mail address:* qxz1@psu.edu (Q.M. Zhang).

0924-4247/$ – see front matter © 2012 Elsevier B.V. All rights reserved.
http://dx.doi.org/10.1016/j.sna.2012.05.002

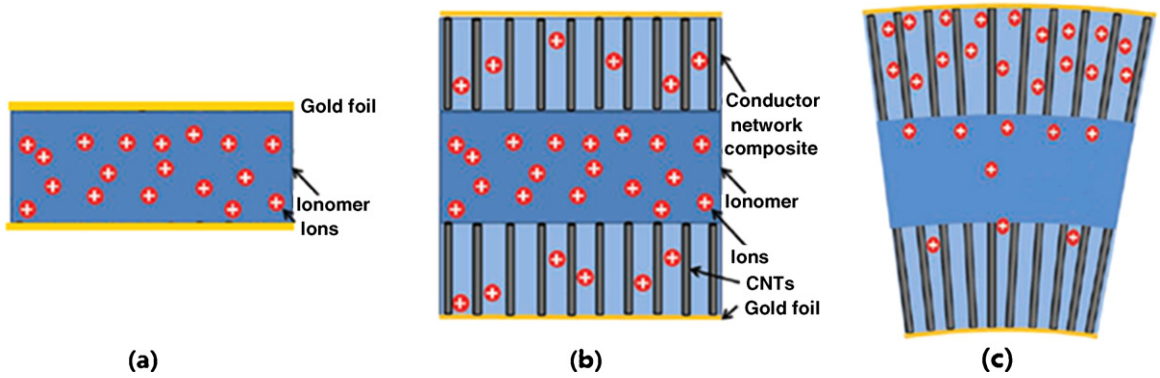


**Fig. 1.** Schematic of (a) *i*-EAP membrane actuator, (b) IPCNC actuator, and (c) actuation mechanism of IPCNC actuator.

in Fig. 1(c), the accumulation or depletion of excess ions at the two electrodes generates the strain response; therefore a high maximum concentration and a fast increase in concentration of excess ions at the electrode regions are highly desired. Further optimization of the actuators critically depends on understanding and quantifying these processes. In electrochemical devices, equivalent circuit models have been widely used to analyze the device performance where they provide understandings on how various components contribute to the device performance. In this study, we introduce equivalent circuit models to analyze the electric impedance spectra of three types of ionic actuators, which can be easily obtained by using a standard impedance analyzer. The actuators studied include: (i) an ionomer membrane actuator consisting of a 25 μm thick Nafion membrane with planar Au electrodes and swelled with 40 wt% of 1-ethyl-3-methylimidazolium trifluoromethanesulfonate (EMI-Tf), referred to as the "membrane actuator" and two state-of-the-art IPCNC actuators; (ii) an IPCNC with the conductive network composite (CNC) electrodes fabricated by a layer-by-layer (LbL) self-assembly process, referred to as the "LbL actuator"; (iii) an IPCNC with a vertically aligned carbon nanotube (VA-CNT) array CNC electrodes, referred to as the "VA-CNT actuator" in this paper. Compared with simple membrane actuators, the IPCNCs in (i) and (ii) possess larger electrode surface areas, and thus exhibit higher bending actuations. The actuator dimensions and their configurations are summarized in Table 1.

In the past decades, a great deal of efforts has been devoted to investigate the charge dynamics in ionic electroactive devices such as *i*-EAP actuators and supercapacitors. The Electrode Polarization (EP) model [13], based on the analysis of electric impedance spectra of ion containing membrane, has been widely used to describe the electric double layer (Stern layer) in ionic membrane, which generally forms within milliseconds [14] and is on the order of nanometer thickness near the charged electrodes (~ the Debye length $\lambda_D$)

$$\lambda_D = \left(\frac{\varepsilon\varepsilon_0 kT}{Z^2 q^2 n}\right)^{1/2} \quad (1)$$

where $Z$ is the mobile ion charge (= 1 for the ionic liquids, EMI-Tf, investigated here), $\varepsilon$ is the relative dielectric constant of the ionic liquids, $\varepsilon_0$ is the dielectric constant of vacuum, $k$ is Boltzmann's constant, $T$ is temperature, $q = e$ (electron charge) and n is the mobile charge concentration. For the ILs, $n = n_+ = n_-$ is assumed. This EP model can be expressed schematically as a RC circuit as illustrated in Fig. 2(a), where $R = d/\sigma S$ and $C = \varepsilon\varepsilon_0 S/\lambda_D$. Here, $d$, $\sigma$, and $S$ are the thickness, conductivity, and area of the ionomer membrane actuator, respectively.

In this paper, we show that although this simple EP model can fit the data for the ionomer membrane actuator well at frequencies above 1 kHz, it cannot describe the low frequency (or long time) response of ions or ion containing polymeric systems under electric stimulus. In fact, the electromechanical responses of *i*-EAP actuators occur at this low frequency range, often at frequencies below 10 Hz. In order to quantify the low frequency ionic responses (diffusion process), the Warburg impedance element, a constant phase element (CPE) that is commonly used to represent diffusion controlled charge transfer process in pseudo-capacitors, should be added to the EP circuit elements (see Fig. 2(b)). Although compared to a pseudo-capacitor, an ionomer with ILs has little redox reaction under low voltage (~0.1 V), we have shown in a previous study that the ion diffusion dominates the electric response above the time scale of milliseconds [14], and here we demonstrate that the equivalent circuit with Warburg impedance element can fit the impedance spectra for *i*-EAP membranes with ILs very well for the entire frequency range. Moreover, it is found that the equivalent circuit with Warburg impedance element can also be used to fit the impedance spectra for IPCNC actuator systems with thin CNC layer such as the IPCNC with LbL actuators which have CNC layer thickness ~64 nm. But for the VA-CNT actuators, the CNC layer thickness is as thick as 12 μm, therefore the ion transport and storage in the composite electrodes have to be taken into consideration in the modeling. It is found that a simplified transmission line circuit, a concept analogous to the De Levie transmission line model to describe the transport of ions in porous electrodes, should be used to describe the CNC layer. The fitting results show that in the VA-CNT actuators, the charge diffusion process becomes comparably less significant and hence by properly controlling the nano-morphology of the CNCs, an *i*-EAP actuator with fast response can be achieved, which was indeed observed in an earlier study [15].

## 2. Experimental

This study employed Nafion™ NR 211 ionomer and two IPCNCs fabricated with Nafion™ NR 211 ionomer as the base material systems for the investigation. Nafion™ NR 211 ionomer membranes were purchased from Aldrich and directly fabricated into

**Table 1**
Summary of dimensions of *i*-EAP actuators.

| | Width (mm) | Length (mm) | Membrane thickness (μm) | CNC thickness (μm) | Total thickness (μm) |
|---|---|---|---|---|---|
| Nafion | 1 | 8 | 25 | 0 | 25 |
| LBL | 1 | 8 | 25 | 0.064 | 25.13 |
| CNT | 0.5 | 8 | 25 | 12 | 49 |

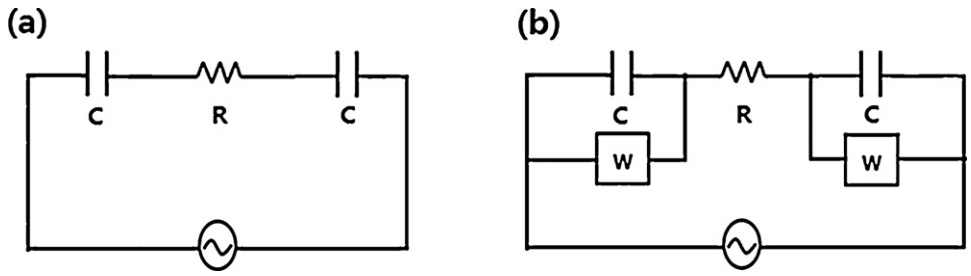


**Fig. 2.** (a) RC equivalent circuit and (b) equivalent circuit with Warburg element.

membrane actuators. The two IPCNCs actuators were fabricated by LbL self-assembly process [8,16] and by integrating vertically aligned carbon nanotube (VA-CNT) forest/ionomer composites onto the ionomer [15], respectively.

The IPCNCs with LbL composites were fabricated by alternately immersing the Nafion film into two aqueous solutions containing PAH as the polycation and anionic gold nanoparticles (Au NP) (3 nm diameter, Purest Colloids Inc.) for 30 times to achieve 30 bilayers of PAH/Au NP CNC. The composites grew via the electrostatic force between PAH and the Au NPs [8,16]. The lateral dimensions of the IPCNCs studied here were 1 mm × 8 mm with a 64 nm thick CNC on each side and a total thickness of approximately 25 μm [17].

The VA-CNT CNCs were fabricated by infiltrating the Nafion solution into densified carbon nanotube forests. CNTs were grown using a modified chemical vapor deposition (CVD) method on silicon substrates using a Fe-on alumina catalyst system [18,19]. The as-synthesized CNTs (1% volume fraction (1 $V_f$%)) originally have densities of $10^9$–$10^{10}$ CNTs/cm$^2$. Via mechanical densification, 10 $V_f$% was obtained for the device under study. Commercial Nafion dispersion purchased from Ion-Power was diluted by dimethylformamide (DMF) and then the solution was infiltrated into CNT arrays under vacuum. After removing the solvent, the composite was annealed at 130 °C under vacuum for 1 h to increase the crystallinity of Nafion. The fabricated VA-CNTs/Nafion nanocomposites were embedded in an epoxy resin and then sectioned at liquid $N_2$ temperature using a finesse microtome with VA-CNTs perpendicular to the cutting direction. Finally, two VA-CNT/Nafion CNC thin layers were bonded to the two sides of the neat Nafion membrane by an ultrathin layer of Nafion dispersion. The stacks were dried and further annealed at 130 °C to improve the bonding. The final device had a lateral size of 0.5 mm × 8 mm and a total thickness of 49 μm, including 25 μm of Nafion and 12 μm of CNC on each side of the Nafion membrane.

40 wt% of 1-ethyl-3-methylimidazolium trifluoromethanesulfonate (EMI-Tf) was soaked into the Nafion NR 211 ionomer membrane and two IPCNC actuators at 60 °C. The uptake of the ionic liquid within the Nafion membrane was calculated from measuring the weight gain after swelling. After achieving 40 wt% uptake, 50 nm thick gold electrodes (L. A. Gold Leaf) were hot-pressed on two sides of actuator surfaces to increase the surface conductivity.

The electrical characteristics were measured in air by a potentiostat (Princeton Applied Research 2273) with 2-electrode settings. In terms of actuation, a DC step voltage was applied on the IPCNC samples and the time resolved electromechanical response of the actuators in air was recorded by using a probe station (Cascade Microtech M150) equipped with a Leica microscope and a CCD camera (Pulnix 6740CL).

## 3. Results and discussion

Presented in Fig. 3 are bending actuations of the three actuators after 1 s of application of 4 V. It can be seen that the bending actuation increases progressively from Fig. 3(a)–(c). The equivalent

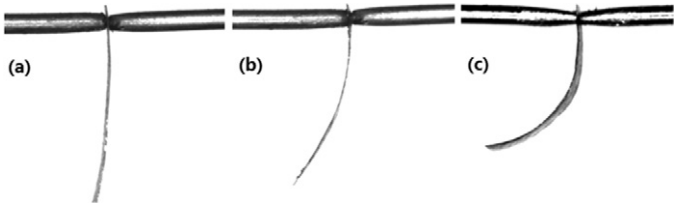


**Fig. 3.** Bending actuation of (a) Nafion, (b) LBL Au/PAH actuator and (c) VA-CNT/Nafion actuator under 4 V for 1 s.

circuit analysis will show that such an increase is caused by an increase in the electrode areas as well as a comparably reduced contribution from the ion diffusion, which is a slow process in the IPCNCs studied.

### 3.1. The ionomer membrane actuator

Presented in Fig. 4(a) and (b) (dashed curves) are the fittings of the electric impedance magnitude and phase of the Nafion membrane actuator using the EP model (Fig. 2(a)). It is obvious that although the model can fit the impedance spectrum well at frequencies above 100 Hz, it deviates significantly from the data at lower frequencies. It should be noted that the resistive element $R$ can be easily determined from the real part of impedance data at high frequencies (>50 kHz) where the imaginary part of the impedance is linked to the electric double layer capacitor element $C_{dl}$. The fitting with simple RC circuit (dashed curves) implies that the low frequency response of this system intrinsically differs from the behaviors of either resistors or capacitors. A diffuse layer [20] continuously contributes to the charging and discharging current so that the system behaves more lossy than an ideal RC circuit. To describe the contribution of the diffuse layer, a Warburg element [21–23] is introduced in parallel with the electric double layer capacitance $C_{dl}$ in Fig. 2(b), as the total stored charge is the sum of the electric double layer charges and the diffuse layer charges [24]. The diffusion process here is assumed as a semi-infinite linear diffusion, that is, unrestricted diffusion to a planar electrode. The Warburg element has an explicit expression as $Z_W = A_W/(j\omega)^{0.5}$, where $A_W$ is the Warburg coefficient [21–23]. A much improved

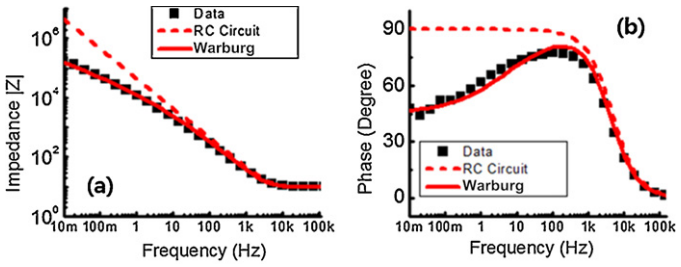


**Fig. 4.** (a) Impedance magnitude and (b) phase of Nafion with 40 wt% EMI-Tf fitted by simple RC circuit and equivalent circuit with Warburg element.

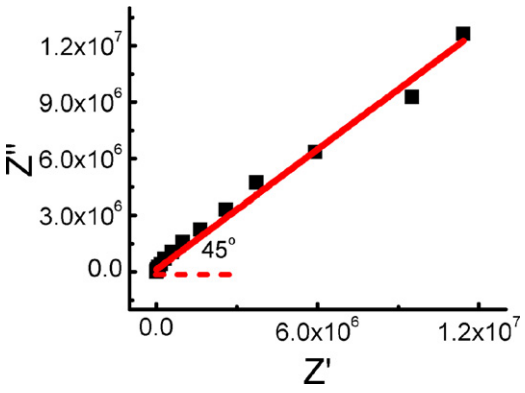


**Fig. 5.** Nyquist plot of Nafion with 40 wt% EMI-Tf.

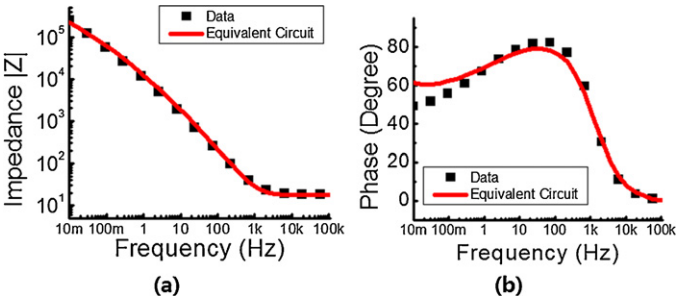


**Fig. 6.** (a) Impedance magnitude and (b) phase of Nafion with LbL Au/PAH composite actuator.

fitting (solid curves) from the equivalent circuit with the Warburg element (Fig. 2(b)) is presented in Fig. 4(a) and (b), where the electric double layer capacitance $C_{dl}$ is 7.5 μF/cm$^2$, the bulk resistance $R$ is 9.7 Ω cm$^2$ and the Warburg coefficient $A_W$ is $10^5$ Ω cm$^2$ s$^{-1/2}$, respectively. To demonstrate the dominance of the diffusion contribution to the charging and actuation response, we present in Fig. 5 the Nyquist plot. It is clear that at low frequencies, the Nyquist plot of the system has 45° phase angle, indicating the dominance of the Warburg impedance over the electric double layer capacitance.

We would like to point out that besides the impedance spectroscopy (frequency domain analysis), a time domain analysis where the charge responses under a step voltage is measured can also be utilized to identify the drift and diffusion process and to determine the electric double layer capacitance in Fig. 2(a) [14]. In general, charge transport is a result of drift and diffusion and can be described by Poisson–Nernst–Planck equations.

$$\varepsilon\varepsilon_0 \frac{\partial E}{\partial x} = \rho \tag{2}$$

$$\psi_{\pm} = \pm\mu n_{\pm} E - D\frac{\partial n_{\pm}}{\partial x} \tag{3}$$

where $\rho$ is the charge concentration, $\varepsilon$ is the dielectric constant of the medium, $\varepsilon_0$ the vacuum permittivity, $\psi$ is the ion flux density, $\mu$ is the ion mobility, n is the ion concentration (the subscripts + and − indicate positive and negative charges), $E$ is the electric field, and $D$ is the diffusion coefficient. For the ionic liquids studied here, we assume $n_+ = n_-$. $\mu$ and $D$ are related by the Einstein equation, $D = \mu KT/q$ [24–26]. For the membrane actuator of Fig. 1(a) under a step voltage, the initial transient current that occurs before the screening of the electric field is $I_0 = V/R$. When the applied voltage is not high, this current follows the charging of the electric double layer capacitors $C$ in series with a bulk resistor $R$ (see Fig. 2(a)) [14,24,27,28],

$$I(t) = I_0 \exp\left(\frac{\tau}{\tau_{dl}}\right) \tag{4}$$

where $\tau_{dl} = RC$. The fitting of the current in the time domain analysis of the membrane actuator yields a $\tau_{dl} = 2.66 \times 10^{-4}$ s and $C = 3.5$ μF/cm$^2$ since $R$ can be independently determined from $I_0$. This result is consistent with the capacitance fitted from the impedance spectroscopy, where $C$ is the total capacitance of the electric double layer capacitance $C_{dl}$ at two electrolyte–electrode interfaces.

### 3.2. The IPCNC actuators

To enhance the performance of *i*-EAP membrane actuator, an IPCNC, which is a composite of an ionic conductor and electronic conductor, is commonly coated on the membrane to increase the electrode surface area, and hence the ion storage for strain generation. A previous study has shown that the actuation magnitude gradually increases with CNC thickness, when the CNC is fabricated by a well-controlled method that results in a controlled morphology [17].

For the LbL actuators, it was found that the equivalent circuit of Fig. 2(b) can fit the data well in the entire frequency range, which indicates that the contribution of the charge transport within the composite electrodes to the actuation is negligible due to the thinness of the CNC layer (~64 nm). However, the significantly increased capacitance $C_{dl}$ (11.4 μF/cm$^2$) results in a large increase in the actuation, while $A_W$ ($1.1 \times 10^5$ Ω cm$^2$ s$^{-1/2}$) is almost the same as that in *i*-EAP membrane actuator. As a result, the actuation speed, which is directly driven by the ion migration, is improved due to the increase in fast actuation component, i.e. the electric double layer capacitance $C$. It explains why LbL actuators achieve fast response as reported previously [17]. Fig. 6(a) and (b) shows the fitting of impedance and phase of LbL IPCNC actuator.

When CNC layer becomes very thick (~12 μm), the lumped equivalent circuit model (Fig. 2(a) and (b)) is no longer adequate to describe the system. A De Levie transmission line model [29] is generally used to describe the electrical response of the porous electrodes by assuming homogeneous pore distribution. As shown in Fig. 7(b), for the Nafion membrane with VA-CNT/Nafion composite actuators, the complicated De Levie transmission line model (Fig. 7(a)) is simplified into a capacitors and resistors network to illustrate the physical meaning of circuit components and also to minimize the fitting parameters. This network consists of two phases, i.e. the electrical conductor phase and the ionic conductor phase, with resistance within each phase and capacitances between the two phases. $C_1$ is the interface resistance between the ionic liquids in the CNC layer and the gold external electrodes; $C_2$ represents the capacitance between the ionic liquids in the CNC layer and the electrical conductor (CNTs) in the CNC layer; and $C_3$ is the interface capacitance between the electrical conductor (CNTs) and the ionic liquids in the ionomer layer (Nafion). For the conduction of ionic liquids, three resistances show the ionic resistance; one in the composite layer ($R_1$), another one on the interface ($R_2$) and one in the bulk Nafion membrane layer ($R$). The resistance within the CNTs is negligible due to the high conductivity of multi-wall CNT [15]. Warburg elements are included to represent the diffusion portion of the electrolyte in the network. The data and fitting of CNT actuator is shown in Fig. 7(c) and (d). All fitting parameters for *i*-EAP actuators discussed are listed in Table 2 for comparison.

As displayed in Table 2, compared to the Nafion membrane, the LbL coating effectively increased the surface area of the electrodes so that the electric double layer capacitance increased from 7.5 μF/cm$^2$ to 11.4 μF/cm$^2$. A much more extended electrode surface area by introducing CNTs further improved the electric double layer capacitance to as high as 3480 μF/cm$^2$. This value is ~460 times greater than that from a planar electrode, which indicates

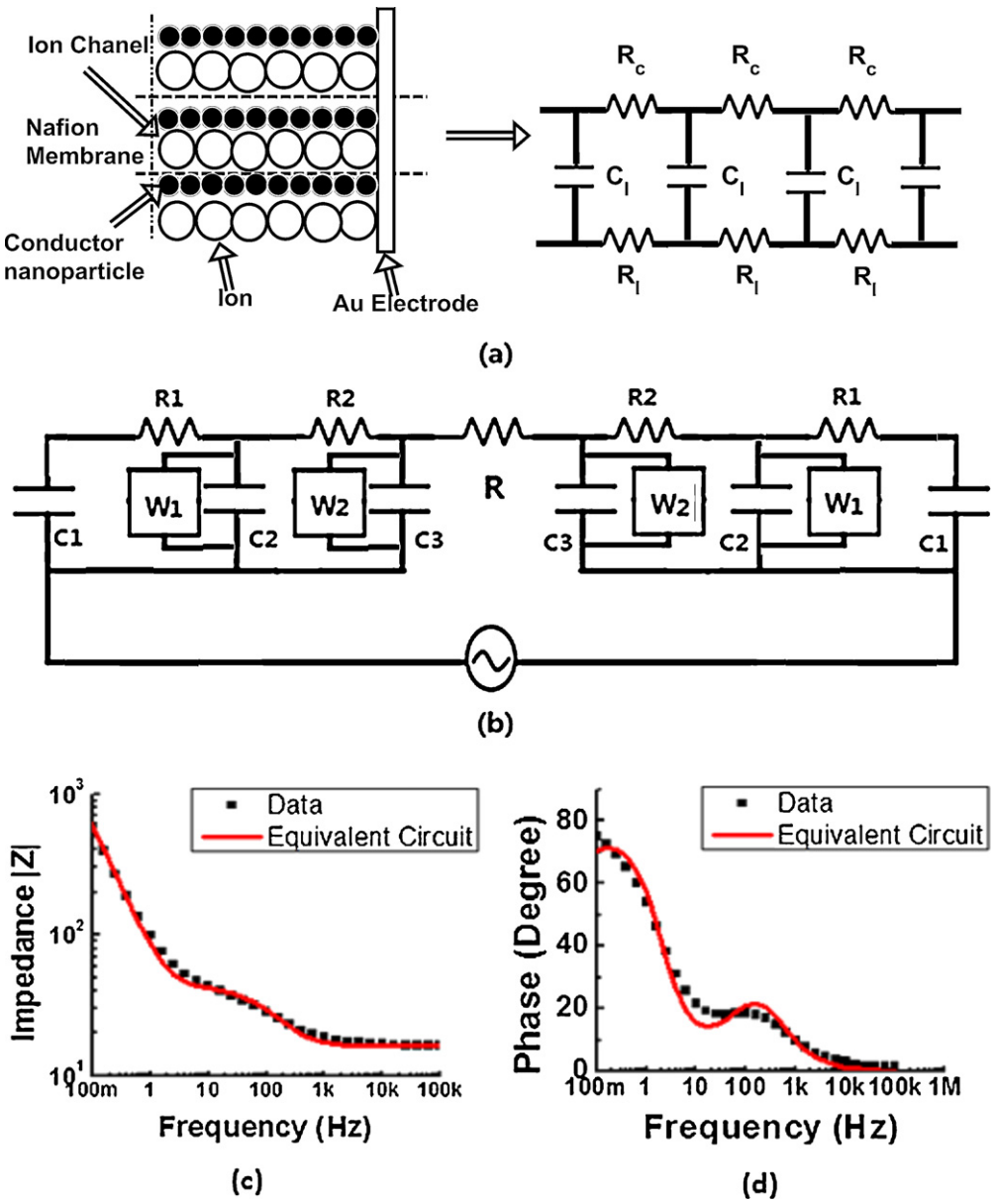


**Fig. 7.** (a) De Levie transmission line model. (b) Equivalent circuit of CNT actuators; Data and fittings of (c) impedance magnitude and (d) phase of VA-CNT actuators.

a 460 times increment in the electrode surface area. Meanwhile, the bulk membrane resistance $R$ in actuators with a CNC is found increased due to the indirect contact between the ionomer and the external electrode, while the Warburg impedances that represent the diffuse layer that built up in the bulk Nafion membrane, remain about the same. Besides the comparison of VA-CNT actuators to the membrane actuators, we would also like to point out that in spite of the large electrode area in the CNC (460 times larger than planar), the Warburg impedance element in the CNC layer $A_{w1}$ is only comparable to that of the diffuse charge on Nafion/CNC interface $A_{w2}$, suggesting a diminishing contribution of the diffusion process to the charge transport in the CNC electrode region. This is consistent with the fact that the spacing between the CNTs in the CNC is only in the range of tens of nanometers which significantly reduces the ion diffusion time ($\sim x^2/D$, where $x$ is the diffusion distance [14,24]) and consequently reduces the contribution of the diffusion process.

The large increase in the electric double layer capacitance of the VA-CNT actuator compared with the relatively minor contribution from the slow diffusion process indicates a significantly increased actuation level with relatively fast speed, both of which were indeed observed in an earlier experimental study [15].

**Table 2**
Fitting parameters for *i*-EAP actuators.

| | | | |
|---|---|---|---|
| Nafion | $C_{dl}$(μF/cm$^2$) | $R$ (Ω cm$^2$) | $A_w$ (Ω cm$^2$ s$^{-1/2}$) |
| | 7.5 | 9.7 | $1 \times 10^5$ |
| LBL | $C_{dl}$ (μF/cm$^2$) | $R$ (Ω cm$^2$) | $A_w$ (Ω cm$^2$ s$^{-1/2}$) |
| | 11.4 | 18.1 | $1.1 \times 10^5$ |
| VA-CNT | $C_1$ (μF/cm$^2$) | $R_1$ (Ω cm$^2$) | $A_{w1}$ (Ω cm$^2$ s$^{-1/2}$) |
| | 35.5 | 12.4 | $1.25 \times 10^5$ |
| | $C_2$ (μF/cm$^2$) | $R_2$ (Ω cm$^2$) | $A_{w2}$ (Ω cm$^2$ s$^{-1/2}$) |
| | 3480 | 15.8 | $1.53 \times 10^5$ |
| | $C_3$ (μF/cm$^2$) | $R$ (Ω cm$^2$) | |
| | 87.9 | 16.3 | |

## 4. Conclusions

In conclusion, equivalent circuits with electric double layer capacitance, bulk ionic resistance and Warburg impedance element are built to model the impedance of *i*-EAP membrane and

IPCNC actuators. We found that the low frequency responses of these devices indicate the presence of ionic diffusion, which is a slow ion transport process. For the neat Nafion membrane actuator, the Warburg impedance element dominates the impedance response at frequencies <100 Hz, consistent with the low actuation speed of the membrane actuators. It was also found that employing proper CNCs in the IPCNC actuators can enhance the electric double layer capacitance while not changing the diffusion component (the Warburg element), which leads to higher strain level and fast strain response.

It was further observed that the equivalent circuit for neat membrane actuator can be used equally well to fit the electric impedance data if the CNC layer is thin, as is the case for the LbL IPCNC actuators. On the other hand, when the CNC layer thickness $\gg\mu$m, an equivalent circuit model with a transmission line should be employed to describe the ion transport in the composite electrode. For the IPCNC actuators with VA-CNT nanocomposite CNC, the significantly enhanced electric double layer capacitance without incurring a large diffusion component (as indicated by the Warburg element) indicates a much large actuation strain generated within the CNC. These results indicate the advantages of IPCNC actuators with properly designed CNC electrodes over the pure ionomer membrane actuators in terms of both the actuation level and response speed.

## Acknowledgments

This material is based upon work supported in part by the U.S. Army Research Office under Grant No. W911NF-07-1-0452 Ionic Liquids in Electro-Active Devices (ILEAD) MURI and by NSF under Grant No. CMMI-1130437. At MIT the work was supported by Airbus S.A.S., Boeing, Embraer, Lockheed Martin, Saab AB, Spirit AeroSystems, Textron Inc., Composite Systems Technology, and TohoTenax Inc. through MIT's Nano-Engineered Composite aerospace Structures (NECST) Consortium. Hülya Cebeci acknowledges support from Scientific and Technical Research Council of Turkey (TUBITAK) for a 2214-International Research Fellowship Programme.

## References

[1] M. Shahinpoor, Y. Bar-Cohen, J.O. Simpson, J. Smith, Ionic polymer–metal composites (IPMCs) as biomimetic sensors, actuators and artificial muscles – a review, Smart Materials and Structures 7 (1998) R15–R30.
[2] W. Lu, A.G. Fadeev, B.H. Qi, E. Smela, B.R. Mattes, J. Ding, G.M. Spinks, J. Mazurkiewicz, D.Z. Zhou, G.G. Wallace, D.R. MacFarlane, S.A. Forsyth, M. Forsyth, Use of ionic liquids for pi-conjugated polymer electrochemical devices, Science 297 (2002) 983–987.
[3] K.J. Kim, M. Shahinpoor, Ionic polymer–metal composites: II. Manufacturing techniques, Smart Materials and Structures 12 (2003) 65–79.
[4] D. Pugal, K. Jung, A. Aabloo, K.J. Kim, Ionic polymer–metal composite mechanoelectrical transduction: review and perspectives, Polymer International 59 (2010) 279–289.
[5] R. Tiwari, E. Garcia, The state of understanding of ionic polymer metal composite architecture: a review, Smart Materials and Structures 20 (2011).
[6] M.D. Bennett, D.J. Leo, Ionic liquids as stable solvents for ionic polymer transducers, Sensors and Actuators A – Physical 115 (2004) 79–90.
[7] J. Wang, C.Y. Xu, M. Taya, A. Y.Kuga, Flemion-based actuator with ionic liquid as solvent, Smart Materials and Structures 16 (2007) S214–S219.
[8] S. Liu, R. Montazami, Y. Liu, V. Jain, M.R. Lin, J.R. Heflin, Q.M. Zhang, Layer-by-layer self-assembled conductor network composites in ionic polymer metal composite actuators with high strain response, Applied Physics Letters 95 (2009).
[9] M. Shahinpoor, K.J. Kim, The effect of surface-electrode resistance on the performance of ionic polymer–metal composite (IPMIC) artificial muscles, Smart Materials and Structures 9 (2000) 543–551.
[10] M. Porfiri, Influence of electrode surface roughness and steric effects on the nonlinear electromechanical behavior of ionic polymer metal composites, Physical Review E 79 (2009).
[11] M. Aureli, W.Y. Lin, M. Porfiri, On the capacitance-boost of ionic polymer metal composites due to electroless plating: theory and experiments, Journal of Applied Physics 105 (2009).
[12] R. Tiwari, K.J. Kim, Effect of metal diffusion on mechanoelectric property of ionic polymer–metal composite, Applied Physics Letters 97 (2010).
[13] R.J. Klein, S.H. Zhang, S. Dou, B.H. Jones, R.H. Colby, J. Runt, Modeling electrode polarization in dielectric spectroscopy: ion mobility and mobile ion concentration of single-ion polymer electrolytes, Journal of Chemical Physics 124 (2006).
[14] J.H. Lin, Y. Liu, Q.M. Zhang, Charge dynamics and bending actuation in Aquivion membrane swelled with ionic liquids, Polymer 52 (2011) 540–546.
[15] S. Liu, Y. Liu, H. Cebeci, R.G. de Villoria, J.H. Lin, B.L. Wardle, Q.M. Zhang, High electromechanical response of ionic polymer actuators with controlled-morphology aligned carbon nanotube/Nafion nanocomposite electrodes, Advanced Functional Materials 20 (2010) 3266–3271.
[16] S. Liu, R. Montazami, Y. Liu, V. Jain, M.R. Lin, X. Zhou, J.R. Heflin, Q.M. Zhang, Influence of the conductor network composites on the electromechanical performance of ionic polymer conductor network composite actuators, Sensors and Actuators A – Physical 157 (2010) 267–275.
[17] R. Montazami, S. Liu, Y. Liu, D. Wang, Q. Zhang, J.R. Heflin, Thickness Dependence of Curvature, Strain, and Response Time in Ionic Electroactive Polymer Actuators Fabricated Via Layer-By-Layer Assembly, AIP, 2011.
[18] S. Vaddiraju, H. Cebeci, K.K. Gleason, B.L. Wardle, Hierarchical multifunctional composites by conformally coating aligned carbon nanotube arrays with conducting polymer, ACS Applied Materials and Interfaces 1 (2009) 2565–2572.
[19] L. Ci, J. Suhr, V. Pushparaj, X. Zhang, P.M. Ajayan, Continuous carbon nanotube reinforced composites, Nano Letters 8 (2008) 2762–2766.
[20] J. Lyklema, Fundamentals of Interface and Colloid Science, Academic Press, 1995.
[21] J.E.B. Randles, Kinetics of rapid electrode reactions, Discussions of the Faraday Society 1 (1947) 11–19.
[22] P. Delahay, New Instrumental Methods in Electrochemistry, Wiley-Interscience, New York, 1954.
[23] A.J. Bard, L.R. Faulkner, Electrochemical Methods: Fundamentals and Applications, 2nd ed., Wiley, 2000.
[24] F. Beunis, F. Strubbe, M. Marescaux, J. Beeckman, K. Neyts, A.R.M. Verschueren, Dynamics of charge transport in planar devices, Physical Review E 78 (2008).
[25] M.Z. Bazant, K. Thornton, A. Ajdari, Diffuse-charge dynamics in electrochemical systems, Physical Review E 70 (2004).
[26] M.S. Kilic, M.Z. Bazant, A. Ajdari, Steric effects in the dynamics of electrolytes at large applied voltages. I. Double-layer charging, Physical Review E 75 (2007).
[27] F. Beunis, F. Strubbe, M. Marescaux, K. Neyts, A.R.M. Verschueren, Diffuse double layer charging in nonpolar liquids, Applied Physics Letters 91 (2007).
[28] M. Marescaux, F. Beunis, F. Strubbe, B. Verboven, K. Neyts, Impact of diffusion layers in strong electrolytes on the transient current, Physical Review E 79 (2009).
[29] R. De Levie, Advances in Electrochemistry and Electrochemical Engineering, Wiley-Interscience, New York, 1967.

## Biographies

**Yang Liu** received her B.S. degree in Physics from University of Science and Technology of China, Hefei, China, in 2004 and received her M.S. degree in Physics from Northeastern University, Boston, MA in 2008. In 2012, she received her Ph.D. from the Department of Electrical Engineering, Pennsylvania State University. Her research interests include electroactive polymers & composites, solid state electromechanical devices, and electric energy storage systems.

**Ran Zhao** received the Bachelor degrees in Materials Science and Engineering from Nanjing University, Nanjing, China, in 2006. She is currently pursuing Master degree in Electrical Engineering, Pennsylvania State University Park. Her research interests include high performance actuators, supercapacitors, and batteries.

**Mehdi Ghaffari** is currently pursuing his Ph.D. degree at the Materials Science and Engineering Department, Pennsylvania State University. His background is in polymer-based devices for energy related applications and his research interest focuses on Electroactive Materials and Energy Harvesting Devices including actuators and supercapacitors based on new generation of carbon materials such as microporous graphene and carbon nanotubes.

**Sheng Liu** received the B.S. degree in Physics from Nanjing University, Nanjing, China, in 2003 and Master degree in Electrical Engineering from Penn State University in 2008. He received his Ph.D. degree in Electrical Engineering from Pennsylvania State University in 2010. His research interests include high performance electroactive polymers and composites devices such as actuators and transducers, ion transport in ionic polymer and composites devices such as supercapacitors and batteries.

**Reza Montazami** is an Assistant Professor of Mechanical Engineering at Iowa State University. He received his B.S. in physics and his M.S. and Ph.D. in Materials Science and Engineering from Virginia Tech. Montazami's research is focused on Smart Materials and Structures with emphasis on polymer-nanoparticle functional thin-films for actuation and sensing applications, to realize nature-inspired soft microrobotics and biomedical devices. His current and previous research projects have been in collaboration with ARL, NRL, NIST, University of Pennsylvania, Pennsylvania State University and Drexel University; and funded through ARL, ASEE and NSF. His current interests are in the areas of biomaterials for biomimetic and biomedical devices, with emphasis on cytotoxicity, biocompatibility and biodegradability of the materials. Montazami has published more than 15 peer-reviewed journal articles and book chapters, and given 8 invited national lectures.

**James R. Heflin** is a professor of Physics at Virginia Tech, where he has been a faculty member since 1992. He received his Ph.D. in Physics from University of Pennsylvania in 1990. He is the Associate Director of the Center for Self-Assembled Nanostructures and Devices at Virginia Tech, an Associate Editor of the International Journal of Nanoscience, and co-editor the textbook "Introduction to Nanoscale Science and Technology." His research focuses on self-assembly of organic optoelectronic materials and devices.

**Qiming Zhang** is a distinguished professor of electrical engineering and materials science and engineering of Penn State University. Dr. Zhang obtained Ph.D. in 1986 from Penn State University. The research areas in his group include fundamentals and applications of novel electronic and electroactive materials. Research activities in his group cover actuators and sensors, transducers, dielectrics and charge storage devices, polymer thin film devices, polymer MEMS, and electro-optic and photonic devices. He has over 330 publications and 14 patents (5 pending) in these areas. His group has discovered and developed a ferroelectric relaxor polymer which possesses room temperature dielectric constant higher than 50, an electrostrictive strain higher than 7% with an elastic energy density $\sim$1 J/cm$^3$. His group also proposed and developed nano-polymer composites based on delocalized electron systems to raise the nano-polymeric composites dielectric constant near 1000. More recently, his group demonstrated a new class of polar-polymer with electric energy density over 25 J/cm$^3$, fast discharge speed and low loss, attractive for high efficiency energy storage capacitors. He is the recipient of the 1999 Penn State Engineering Society Outstanding Research Award and a fellow of IEEE.